

APPLICATION OF NONLINEAR REGRESSION IN THE ANALYSIS OF RELAXATION PHOTOCURRENT WAVEFORMS

Witold Kaczmarek, Marek Suproniuk, Karol Piwowski, Bogdan Perka, Piotr Paziewski

Institute of Electronic Systems, Department of Electronics, Military University of Technology, ul. gen. Sylwestra Kaliskiego 2, 00-908 Warszawa, Poland (✉ witold.kaczmarek@wat.edu.pl, marek.suproniuk@wat.edu.pl, karol.piwowski@wat.edu.pl, bogdan.perka@wat.edu.pl, piotr.paziewski@wat.edu.pl)

Abstract

This article discusses the performance of an algorithm for detection of defect centers in semiconductor materials. It is based on direct parameter approximation with nonlinear regression to determine the parameters of thermal emission rate in the photocurrent waveforms. The methodology of the proposed algorithm was presented and its application procedure was described and the results of its application can be seen in measured photocurrent waveforms of a silicon crystal examined with *High-Resolution Photoinduced Transient Spectroscopy* (HRPITS). The performance of the presented algorithm was verified using simulated photocurrent waveforms without and with noise at the level of 10^{-2} . This paper presents for the first time the application of the direct approximation method using modern regression and clustering algorithms for the study of defect centers in semiconductors.

Keywords: defect centers, semiconductor materials, nonlinear regression method.

1. Introduction

The performance of semiconductor materials is strongly dependent on their defect structure. In order to ensure better and more accurate parameters of electronic components, it is necessary to know as precisely as possible the defect structure of materials from which new devices are to be made. In order to attain the assumed parameters of these materials, defect centers detection methods of the highest accuracy should be used. This paper presents the principles and results of an algorithm for defect centers detection based on nonlinear regression for the determination of emission rate parameters in simulated photocurrent waveforms and relaxation photocurrent waveforms recorded in the Si crystal with the use of *High-Resolution Photoinduced Transient Spectroscopy* (HRPITS).

2. The use of high-resolution nonstationary HRPITS photocurrent spectroscopy in the study of defect centers.

In the course of the study of defect centers, the measurements of the physical parameters of the semiconductor sample are essential. One of the most effective methods of defect structure determination in high-resistivity semiconductor materials is High-Resolution Photoinduced Transient Spectroscopy [1-4]. It is based on the use of the phenomenon of capture and thermal emission of charge carriers from defect centers in the process of illumination of the sample with a pulse of light. The idea of measuring changes in the conductivity of a sample with the HRPITS method is presented in Fig. 1.

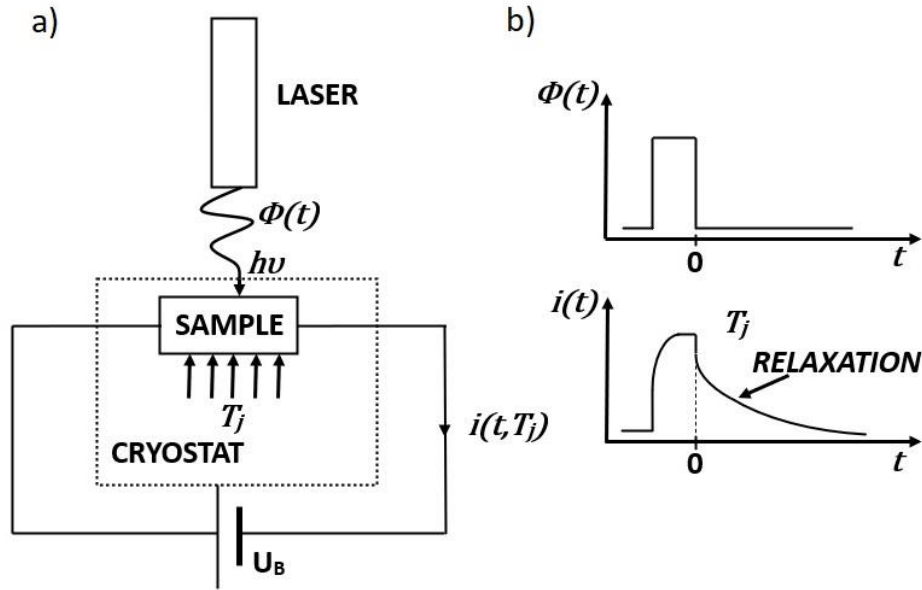


Fig. 1. Idea of measuring changes in the conductivity of a sample with the HRPITS method. Scheme of the measuring system (a) and the light pulse and photocurrent relaxation waveforms (b). Excess charge carriers filling the defect centers are generated by a light pulse $\Phi(t)$ with an energy hu greater than or equal to the width of the energy gap. The relaxation of the photocurrent $i(t)$ after switching off the lighting is the result of thermal emission of charge carriers from defect centers at temperature T_j [1].

During the illumination of the sample, parallel processes of generation and recombination of excess charge carriers take place. When the illumination is turned off, these processes directly affect the concentration of the excess carriers. Due to the fact that the concentration of excess carriers is related to the conductivity of the sample, measuring the conductivity relaxation after turning off the illumination provides information about the processes of thermal emission of carriers from the defect centers. This is due to the fact that thermal emission from defect levels is much slower than recombination processes. The change in sample conductivity as a function of time after illumination with photons of energy greater than the energy gap width can be described as is shown in (1) [1]:

$$\sigma t = q[n t \mu_n + p t \mu_p], \quad (1)$$

where q is the elementary charge, $n t$ and $p t$ are the concentrations of free electrons and holes, and μ_n and μ_p are their mobilities, respectively.

Changes in sample conductivity as a function of time and electric field strength have a direct effect on the photocurrent relaxation for carrier emission from a single defect center. This relationship can be defined by (2):

$$i t = \sigma t C E, \quad (2)$$

where σt is the change in sample conductivity as a function of time, C is the effective cross-sectional area of the sample through which the current flows, and E is the electric field strength depending on the voltage applied to the sample and the distance between the electrodes.

After transformations taking into account the equations describing the processes of generation of free electrons, holes and the concentration of electrons captured by defect centers at a certain temperature, the changes in the conductivity of the sample as a function of time,

after turning off the illumination, can be described by an exponential expression. The relaxation photocurrent waveform for multiple defect centers takes the form of (3) [1, 4-7]:

$$i(t, T) = \sum_{k=1}^K I_k(\lambda, T) \exp[-e_{T_k} T t], \quad (3)$$
$$k = 1 \dots K,$$

where I_k are relaxation amplitudes dependent on temperature T and the wavelength of light λ incident on the sample, e_{T_k} determines the rate of emission of carriers from the k -th defect center at a given temperature. Taking into account the fact that we use a light source of a specific wavelength during the measurements, the wavelength has no influence on the photocurrent.

The measurements in a wide range of temperatures allow for the approximation of the $e_{T_k} T$ dependence with the Arrhenius equation taking the form of (4) [1, 3-10]:

$$e_{T_k} = A_k T^2 \exp\left(-\frac{E_a}{k_B T}\right), \quad (4)$$

where A_k is a constant depending on the properties of a given defect center, E_a is its activation energy and k_B is Boltzmann's constant. Thus, in order to determine the parameters of the defect centers from the relaxation photocurrent waveforms measured with the HRPITS method, the values of the parameters A_k and E_a must be calculated from the equation above.

3. Direct approximation method in the process of defect center parameters determination based on the results of nonstationary photocurrent spectroscopy

There are many methods for defect center identification. One of less popular methods of defect centers determination is the direct approximation procedure, which involves determination of current parameters and emission rates directly from the signal measured at a given temperature. The greatest advantage of direct approximation is the ease of interpretation of the obtained results, due to their unambiguous character. The parameters obtained by direct approximation can therefore be used for further calculations in the process of defect center identification. The main problem in this method is to find an algorithm that will adjust the number of exponents of the defined function so that they correspond to the real number of exponents in the measured signal. In addition, the approximation algorithm itself may introduce additional errors that can prevent correct estimation of parameters of exponent functions. Selection of proper approximation algorithm is therefore crucial to obtain reliable results, allowing for identification of specific defect centers.

In a previously conducted study, the effectiveness of nonlinear regression algorithms was tested in the process of determining the component parameters of the expository functions. The obtained results made it possible to assume that nonlinear regression algorithms can calculate the component parameters of the exposure functions in a very accurate way, even in noisy signals [4]. The information above allowed us to create a method for studying defect centers using nonlinear regression algorithms.

To test the effectiveness of the direct approximation method, a program was written in the PYTHON language. As this language is commonly used to solve many mathematical problems [11], it is possible to use ready-made function implementations allowing to realize the idea contained in the procedure diagram presented in Fig. 2.

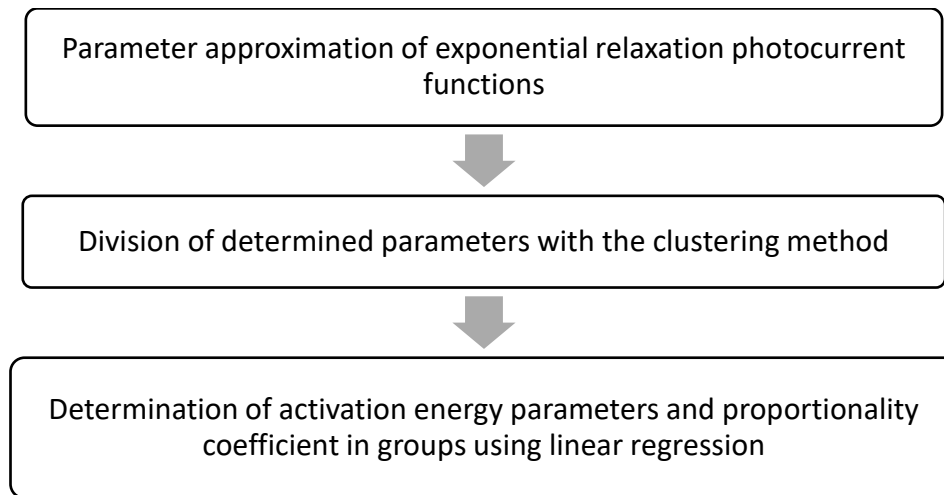


Fig. 2. Schematic of the direct approximation method.

In the first step of the calculations, the curve fit function is used to perform a nonlinear regression with the Trust Region Reflective algorithm [12-13]. This algorithm is characterized by the possibility of introducing boundaries within which the component parameters are to be searched. This makes it possible to automatically reject results that do not make physical sense. To select the optimal form of the approximating function, the algorithm is replayed in a loop a certain number of times, with values for the increasing number of exponentiated component functions being computed at each successive step. This makes it possible to quickly check the degree of fit of the approximation to the given signal. In order to choose the best form of the approximation function, in each step the mean square error is calculated as a sum of squares of differences between points at a given moment of time in the tested waveform and values for these moments in the approximated waveform. Such estimation acceptably works as a classifier of the degree of fit of the calculated parameters to the true values. Figure 3 shows the calculated emission rate parameters as a function of temperature for the Si crystal.

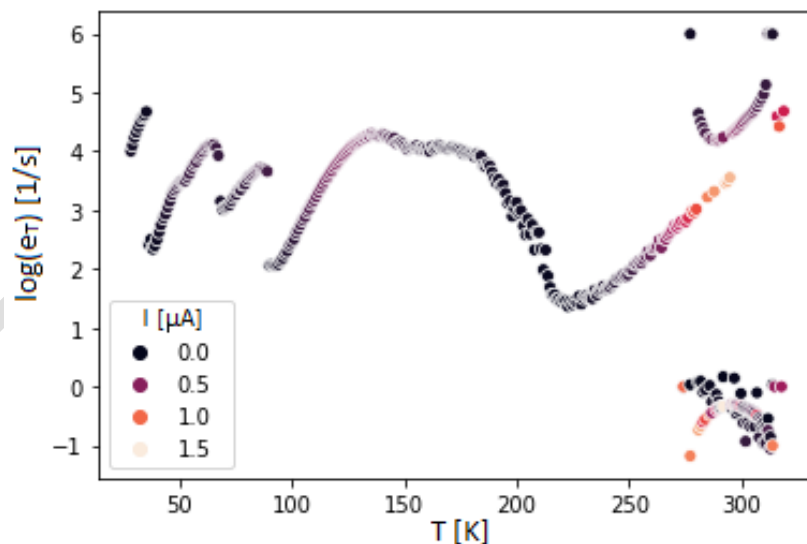


Fig. 3. Emission rate parameters as a function of temperature detected in silicon Si crystal using direct approximation method.

In the next step, the determined parameters are divided into groups using the *Density-based Spatial Clustering of Applications with Noise* (DBSCAN) function [14, 15]. This function, on

the basis of given pair-meter distances to neighboring samples, classifies them into groups. Additionally, after the initial division, it is checked if there are no symptoms of the presence of more defect centers in a given group. A sign of such a situation is a visible change in the trend of a given group. In order to check whether the group should be divided, a check of the percentage increase of consecutive samples in the group is carried out. If three consecutive samples show a significant change in trend, the cluster is split. In order to prevent splitting of the group in which there is significant noise, we check the size of newly determined clusters. If they are too small, they are not classified as separate groups and the studied cluster remains in its original form. The clustering allows to determine the parameters of specific defect centers and to discard samples that could significantly distort the results. Figure 4, shows the results of the clustering algorithm.

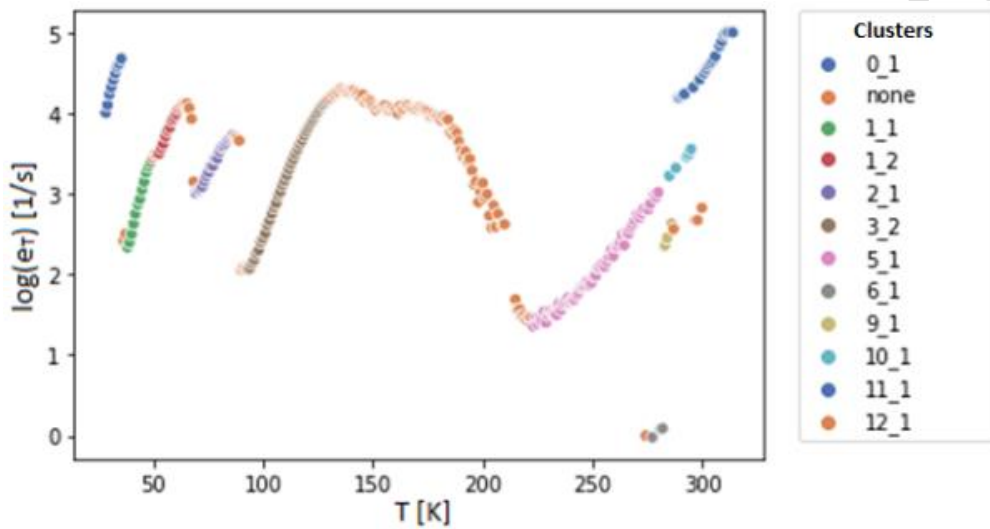


Fig. 4. Clusters of emission velocity parameters as a function of temperature.

In the last step of the calculation, the calculated parameters are projected in the coordinate system $[x = \ln(T^2/eTk), y = 1000/T]$ and approximated with linear regression method, using the OLS (ordinary least squares) function.

A depiction of the last step of the algorithm can be seen in Fig. 5.

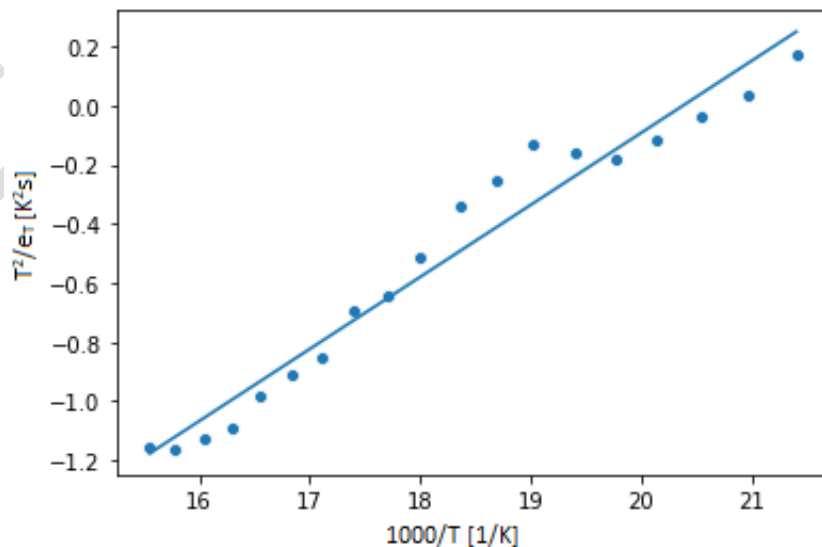


Fig. 5. Straight line determined from the operation of the OLS function in Cluster Group 1_2.

According to the directional equation of the line (5), this function allows us to calculate the parameter a_k , which defines the angle of inclination of the line with respect to the x-axis, and b_k , which denotes the offset of the line on the y-axis.

$$y = a_k x + b_k \quad (5)$$

In addition, the OLS function calculates the approximation error, which is necessary to determine the accuracy of parameter approximation. The operation above enables the calculation of parameters from the transformed Arrhenius (6) [1].

$$\frac{1}{T} = \frac{k_B}{E_a} \cdot \ln\left(\frac{T^2}{e_T}\right) + \frac{k_B}{E_a} \cdot \ln A . \quad (6)$$

From the equation above, the activation energy of the E_{ak} center is calculated from the parameters of the determined straight line (7) [1]

$$E_{ak} = 10^3 \frac{k_B}{a_k} \quad (7)$$

and the value of the A_k factor (8) [1].

$$A_k = \exp\left(\frac{b_k}{a_k}\right). \quad (8)$$

As a result of implementing the described algorithm, the parameters of the defect centers for the Si silicon crystal were determined and verified using a simulated run.

4. Verification of the performance of the proposed method using simulated photocurrent waveforms

To verify the effectiveness of the proposed method, the algorithm was tested using simulated photocurrent waveforms. Equation (3) shows that the value of a single component of the exponential function can be described by (9) [16]:

$$i(t) = I_0 \exp(-e_T t) , \quad (9)$$

where I_0 is described by Equation 10:

$$I_0 = q N_T \mu_n \tau_n E C e_T \quad (10)$$

in which q is the elementary charge, N_T the concentration of traps, $\mu_n \tau_n$ the product of mobility and lifetime of electrons, E the electric field strength causing the lift of electrons emitted from traps, C the cross-sectional area of the region where thermal emission of electrons occurs and e_T the rate of emission of electrons from a particular defect center.

Based on the above equations and the Arrhenius equation, it is possible to transform (3) to the form:

$$i(t, T) = \sum_{k=1}^K q N_{T_k} \mu_{nk} \tau_{nk} E C A_k T^2 \exp\left(-\frac{E_a}{k_B T}\right) \cdot \exp\left[A_k T^2 \exp\left(-\frac{E_a}{k_B T}\right) t\right], \quad (11)$$

$$k = 1 \dots K$$

The equation above allows to simulate the photocurrent waveforms at different temperature ranges, based on the assumed parameters of the product of electron mobility and lifetime, trap concentration, electric field strength, activation energy and proportionality coefficient, for each defect center separately.

In addition, to check the effectiveness of the method for measurement results whose parameters are uncertain, Equation 12 was derived from Equation 10:

$$K = \frac{I_0}{e_T}, \quad (12)$$

where the parameter K is described by Equation 13:

$$K = N_T \mu_n \tau_n q E C. \quad (13)$$

The values of the product of I_0 and e_T are calculated during the operation of the nonlinear regression algorithm on the basis of the results obtained during testing of experimental samples. During the simulation, the K parameter was calculated for selected samples at temperatures where only one defect center is visible.

In addition, to check the performance of the method under different conditions, the simulated waveforms have been noised according to (14):

$$i_{noise} t, T = i_{sym} t, T + [i_{sym} t, T \cdot rand[0; 1] \cdot p_{noise}], \quad (14)$$

where $i_{sym} t, T$ is the simulated photocurrent signal, $rand[0; 1]$ is a pseudo-random variable from 0 to 1, and p_{noise} is a variable to parameterize the magnitude of the noise relative to the signal level.

The result of applying the direct approximation method to the unnoised waveforms simulated from the detected defect centers in the silicon sample is shown in Fig. 6.

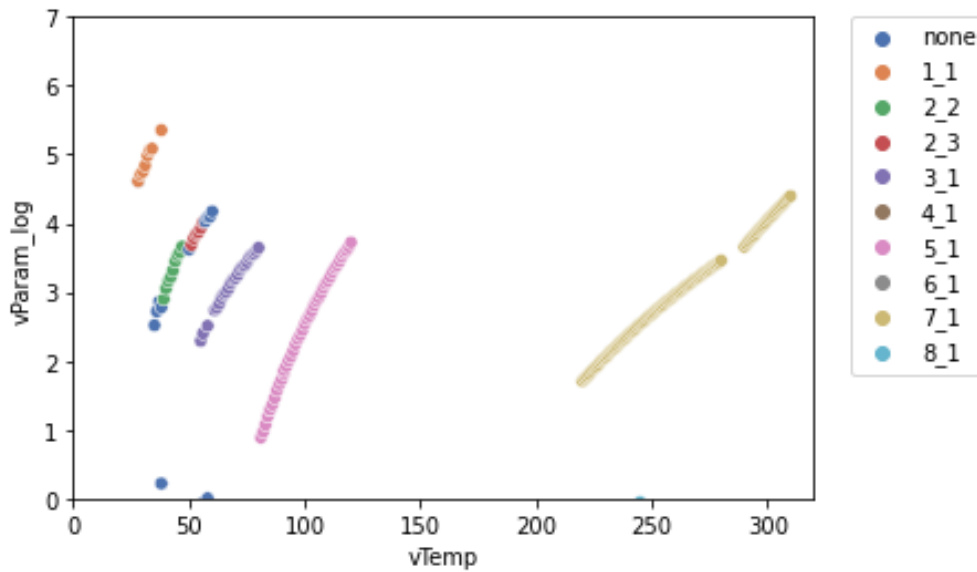


Fig. 6. Result of applying the direct approximation method to the simulated signal based on the obtained parameters from the Si silicon sample.

5. Results

During the testing of the silicon sample, the results described in Table 1 were obtained.

Table 1. Defect centers detected using the direct approximation algorithm.

Defect Center	E_a (meV)	A ($K^{-2}s^{-1}$)	$A_{min}-A_{max}$ ($K^{-2}s^{-1}$)
T0	14±1	451932	235188-944052
T1	31±1	215724	175151-268517
T2	29±1	72560	53284-102540
T3	41±1	21087	17465-25623
T4	132±1	1.51×10^7	$(1.34-1.70) \times 10^7$
T5	336±10	1.14×10^7	$(0.70-1.92) \times 10^7$
T6	632±33	1.59×10^{12}	$(0.48-5.97) \times 10^{12}$

These parameters were used to simulate the waveforms in order to validate the performance of the proposed method. The parameters obtained in the process of evaluating the results using the simulated runs are shown in Tables 2 and 3.

It can be concluded from the previously presented tables that the direct approximation method performs very well in determining the parameters of activation energy and proportionality coefficient in defect centers. The differences in the results between the performance of the method on the studied waveforms and the simulated waveforms are due to the inaccuracy of reproducing the physical waveforms in the simulation. This is due to problems with accurate estimation of the parameter K , which for the simulation was for the following defects equal to: 5.73×10^{-6} for T0, 1.26×10^{-4} for T1, 6.83×10^{-5} for T2, 6.64×10^{-5} for T3, 5.24×10^{-4} for T4, 2.13×10^{-3} for T5 and 3.53×10^{-4} for T6.

Introducing noise with a p_{noise} parameter of 10^{-2} did not significantly change the estimated results. In case of non-noised signal T5 and T6 defects were qualified to one group during the operation of the clustering function. In the case of the noiseless signal such situation did not occur. This is most likely due to the fact that DBSCAN groups the samples on the basis of the distance vector from the previous ones. It can be assumed that the grouping function based on the distance from the given curve would be more accurate and could increase the accuracy of calculations.

Table 2. Defect centers detected by simulated noise-free waveforms.

Defect Center	E_a (meV)	A ($K^{-2}s^{-1}$)	$A_{min}-A_{max}$ ($K^{-2}s^{-1}$)
T0	11±3	231842	235188-645780
T1	27±2	181023	47848-71434
T2	26±4	72227	37456-106778
T3	35±3	11855	7687-25623
T4	123±4	1.12×10^7	$(0.98-1.88) \times 10^7$
T5	334±13	6.95×10^6	$(0.56-1.92) \times 10^7$

Table 3. Defect centers detected in simulated noise with a noise parameter of 10^{-2} .

Defect Center	E_a (meV)	A ($K^{-2}s^{-1}$)	$A_{min}-A_{max}$ ($K^{-2}s^{-1}$)
T0	15±2	290599	208930-1057630
T1	28±3	225592	97823-291856
T2	22±3	41532	33543-99012
T3	35±5	11643	9477-19542
T4	134±4	2.13×10^7	$(0.94-3.87) \times 10^7$
T5	314±12	1.68×10^6	$(0.25-2.53) \times 10^7$
T6	606±19	1.68×10^{12}	$(0.25-2.56) \times 10^{12}$

6. Conclusions and Summary

The performance of the direct approximation method was tested on measured and simulated waveforms. The proposed method allows for quite accurate and precise calculation of defect center parameters. The discrepancy in the results between the physical and simulated waveforms is due to the inaccuracy of the K parameter estimation and the impossibility of reproducing the given signals.

The defects calculated from the signals measured during testing of the physical sample were also compared with the results obtained from testing this sample using the inverse Laplace transform method [1], and the calculated values of the parameters of the defect centers were additionally compared with the correlation procedure [17]. A comparison of the results obtained using the proposed algorithm and inverse Laplace transform method is shown in Table 4 and Fig. 7. Table 5 shows the parameters of the defect centers obtained using the correlation procedure.

Table 4. Comparison of parameters of detected defect centers by direct approximation and inverse Laplace transform methods.

Method	Direct approximation			Invers Laplace transform		
	E_a (meV)	A ($K^{-2}s^{-1}$)	$A_{min}-A_{max}$ ($K^{-2}s^{-1}$)	E_a (meV)	A ($K^{-2}s^{-1}$)	$A_{min}-A_{max}$ ($K^{-2}s^{-1}$)
T0	14±1	451932	235188-944052	-	-	-
T1	31±1	215724	175151-268517	62±10	3.41×10^7	$(1.2-11) \times 10^7$
T2	29±1	72560	53284-102540	64±3	2.81×10^6	$(0.75-4.1) \times 10^7$
T3	41±1	21087	17465-25623	106±15	7.06×10^6	$(0.25-1.38) \times 10^7$
T4	132±1	1.51×10^7	$(1.34-1.70) \times 10^7$	162±6	1.25×10^7	$(0.6-1.9) \times 10^7$
T5	336±10	1.14×10^7	$(0.70-1.92) \times 10^7$	-	-	-
T6	632±33	1.59×10^{12}	$(0.48-5.97) \times 10^{12}$	-	-	-

Table 5. Parameters of defect centers detected with the correlation procedure [17].

Method	Correlation procedure			
	Defect Center	E_a (meV)	A ($K^{-2}s^{-1}$)	$A_{min}-A_{max}$ ($K^{-2}s^{-1}$)
T1	T1	64 ± 3	9.00×10^7	$(0.4-1.27) \times 10^8$
T2	T2	70 ± 5	1.70×10^7	$(0.5-2.38) \times 10^7$
T3	T3	110 ± 10	3.72×10^7	$(1.2-11) \times 10^7$
T4	T4	176 ± 7	6.55×10^7	$(1.9-12) \times 10^7$

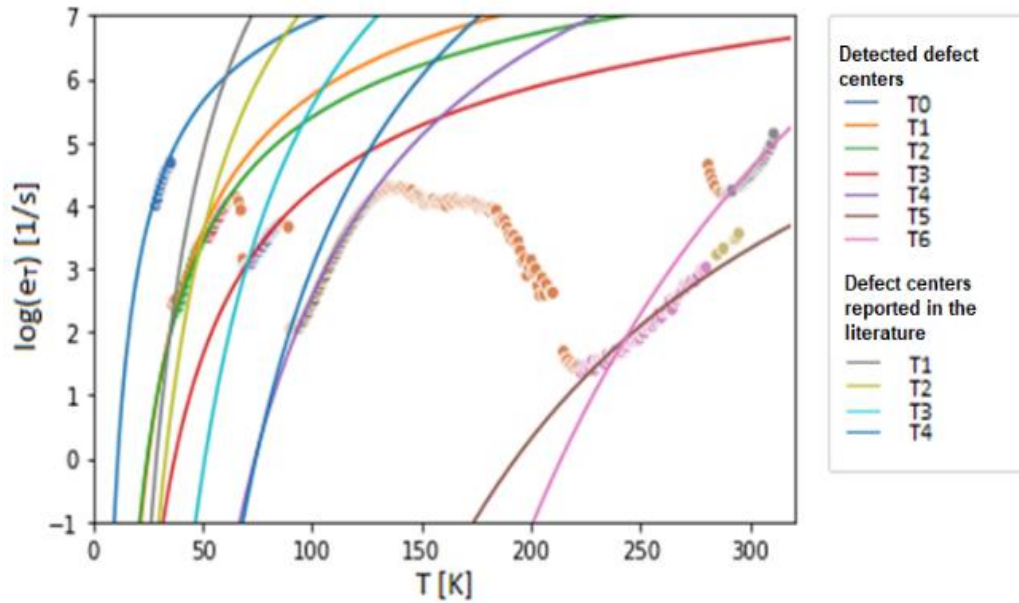


Fig. 7. Defects detected by the algorithm using direct approximation of photocurrent waveforms by nonlinear regression compared with parameters reported in the literature for the inverse Laplace transform method [1].

Based on the data in Table 4 and 5, we can conclude that the accuracy of defect center parameter estimation is higher for the direct approximation method [1, 17, 18]. Attention is drawn to the value of activation energy, which in the case of direct approximation is lower than that calculated with the inverse Laplace transform method and correlation procedure [1, 17]. Based on the comparison of the activation energy values in the simulated signal, it can be assumed that it was estimated quite accurately. In addition, the direct approximation method allows to estimate the value of the proportionality coefficient parameter with much smaller scatter. Thanks to the direct approximation method, it was also possible to observe the symptoms of the occurrence of T0, T5 and T6 centers which were not detected using the inverse Laplace transform or correlation procedure.

The methodology of the proposed algorithm was presented and described. The results of the application of the algorithm for the Si sample were shown and compared with the results available in the literature obtained with the other method. Verification was done using simulated signals with and without noise. The presented algorithm gives the possibility of a more accurate determination of the defect structure of the tested semiconductor material. Since the properties of a semiconductor material depend on its defect structure, its use can be helpful in the development of materials with desired properties, and thus also in the development of new electronic devices. The goal of further work will be to fully automate the proposed algorithm and to increase the accuracy of the measurements by refining the operation of the clustering function.

Acknowledgements

This paper was founded by the grant no. UGB 737/2022. Additionally, the authors would like to thank the team of prof. Paweł Kamiński from the Łukasiewicz Institute of Microelectronic and Photonics for sharing the measurement results of the silicon Si sample tested with the HRPITS method.

References

- [1] Pawłowski, M. (2007). *Obrazowanie struktury defektowej materiałów półizolujących z wykorzystaniem niestacjonarnej spektroskopii fotoprądowej*. Wojskowa Akademia Techniczna.
- [2] Górecki, K., & Górecki, P. (2015). The analysis of accuracy of selected methods of measuring the thermal resistance of IGBTs. *Metrology and Measurement Systems*, 22(3), 455–464.
- [3] Suproniuk, M. (2021). Modelling of changes in the resistivity of semi-insulating materials. *Metrology and Measurement Systems*, 28(3), 581-592.
- [4] Kaczmarek, W., Suproniuk, M., Piwowarski, K., Perka, B., & Paziewski, P. (2021). Porównanie skuteczności algorytmów regresji nieliniowej w procesie identyfikacji centrów defektowych półizolujących materiałów półprzewodnikowych. *Przegląd Elektrotechniczny*, 97(10), 110–113.
- [5] Brasil, M. J., & Motisuke, P. (1990). Deep center characterization by photo-induced transient spectroscopy. *Journal of Applied Physics*, 68(7), 3370-3376.
- [6] Miczuga, M., Kamiński, P., Kozłowski, P., & Kopczyński, K. (2011). Problemy metrologiczne związane z wyznaczeniem koncentracji centrów defektowych w półprzewodnikach wysokorezystywnych o szerokiej przerwie energetycznej. *Pomiary Automatyka Kontrola*, 57, 1368-1371.
- [7] Kozłowski, R. (2000). Wyznaczanie czasu życia nośników ładunku i poziomów rekombinacyjnych w materiałach wysokorezystywnych poprzez pomiar temperaturowej zależności fotoprądu. *Materiały Elektroniczne*, 28(1-2), 5-17.
- [8] Kamiński, P., Kozłowski, R., Krupka, J., Kozubal, M., Wodzyński, M., & Żelazko, J. (2014). Głębokie centra defektowe w krzemie o bardzo wysokiej rezystywności. *Materiały Elektroniczne*, 42(4), 16-24.
- [9] Kamiński, P., Żelazko, J., Kozłowski, R., Hindrichsen, C., & Jensen, L. (2022). Investigation of Energy Levels of Small Vacancy Clusters in Proton Irradiated Silicon by Laplace Photoinduced Transient Spectroscopy. *Crystals*, 12(12), 1703. <https://doi.org/10.3390/cryst12121703>
- [10] Możdżyńska, E. B., Kamiński, P., Kozłowski, R., Korona, K. P., Złotnik, S., Jezierska, E., & Baranowski, J. M. (2022). Effect of the growth temperature on the formation of deep-level defects and optical properties of epitaxial BGaN. *Journal of Materials Science*, 57(36), 17347-17362. <https://doi.org/10.1007/s10853-022-07725-4>
- [11] Kelley, C. T. (1995). *Iterative Methods for Linear and Nonlinear Equations*. SIAM.
- [12] Johansson, R. (2021). *Matematyczny Python: obliczenia naukowe i analiza danych z użyciem NumPy, SciPy i Matplotlib*. Helion.
- [13] Conn, A. R., Gould, N. I. M., & Toint, P. L. (2000). *Trust region methods*. SIAM.
- [14] Delagnes, T., Henneron, T., Clénet, S., Fratila, M., & Ducreux, J. (2023). Comparison of reduced basis construction methods for Model Order Reduction, with application to non-linear low frequency electromagnetics. *Mathematics and Computers in Simulation*, 211, 470–488. <https://doi.org/10.1016/j.matcom.2023.04.007>
- [15] Agapito, G., Milano, M., & Cannataro, M. (2022). A Python clustering analysis protocol of genes expression data sets. *Genes*, 13(10), 1839. <https://doi.org/10.3390/genes13101839>
- [16] Kozłowski, R., Kamiński, P., & Żelazko, J. (2012). Wyznaczanie koncentracji centrów defektowych w półprzewodnikach wysokorezystywnych na podstawie prążków widmowych Laplace'a otrzymywanych w wyniku analizy relaksacyjnych przebiegów fotoprądu. *Materiały Elektroniczne*, 40, 19-33.
- [17] Suproniuk, M., Pawłowski, M., Wierzbowski, M., Majda-Zdancewicz, E., & Pawłowski, M. (2018). Comparison of methods applied in photoinduced transient spectroscopy to determining the defect center

parameters: The correlation procedure and the signal analysis based on inverse Laplace transformation. *Review of Scientific Instruments*, 89(4). <https://doi.org/10.1063/1.5004098>

- [18] Pawłowski, M., Miczuga, M., Kamiński, P., & Kozłowski, R. (2001). Analysis of two-dimensional PITS spectra for characterization of defect centers in high-resistivity materials. *Proceedings of SPIE*. <https://doi.org/10.1117/12.425431>



Witold Kaczmarek received his M.Sc. degree from the Military University of Technology, in 2018. He is currently working toward the Ph.D. degree in electronics. His research activity focuses on semiconductor material properties.



Piotr Paziewski is a research and didactic assistant of Electrical Circuits and Signals Department of the Military University of Technology in Warsaw. He is currently working toward the Ph.D. degree in electronics. His research activity focuses on pulse power systems and energy converters.



Marek Suproniuk received his D.Sc. degree from the Military University of Technology, in 2021. He is currently an associate professor and the Head of Electrical Circuits and Signals Department of the Military University of Technology in Warsaw. His research activity focuses on semiconductor material properties when applied in photoconductive semiconductor switches.



Bogdan Perka received the Ph.D. degree from the Kazimierz Pułaski University of Technology and Humanities in Radom in 2020. He is currently an assistant professor in the Electrical Circuits and Signals Department of the Military University of Technology in Warsaw. His research activity focuses on safety of power and electrical systems.



Karol Piwowarski is a research and didactic assistant of Electrical Circuits and Signals Department of the Military University of Technology in Warsaw. He is currently working toward the Ph.D. degree in electronics. His research activity focuses on pulse power systems and on semiconductor material properties.

Early Access